

Spin-orbit splitting in the $X^2\Pi$, $a^4\Pi$, $B^2\Pi$ and $H^2\Pi$ electronic states of the NS radical

D.H. Shi^a, W. Xing, J.F. Sun, and Z.L. Zhu

College of Physics and Information Engineering, Henan Normal University, Xinxiang 453007, P.R. China

Received 28 March 2012

Published online 10 July 2012 – © EDP Sciences, Società Italiana di Fisica, Springer-Verlag 2012

Abstract. The potential energy curves (PECs) of ten Ω states ($X^2\Pi_{1/2,3/2}$, $a^4\Pi_{1/2,1/2,3/2,5/2}$, $B^2\Pi_{1/2,3/2}$ and $H^2\Pi_{1/2,3/2}$) generated from four Λ -S states ($X^2\Pi$, $a^4\Pi$, $B^2\Pi$ and $H^2\Pi$) of the NS radical are studied in detail for the first time using an ab initio quantum chemical method. All the PEC calculations are performed for internuclear separations from 0.10 to 1.11 nm by the complete active space self-consistent field method followed by the internally contracted multireference configuration interaction approach with the Davidson modifications (MRCI + Q). The spin-orbit coupling (SO) effect is accounted for by the Breit-Pauli Hamiltonian. To discuss the effect on the energy splitting by the core-electron correlations, two all-electron basis sets, cc-pCVTZ and cc-pVTZ, are used for the SO coupling calculations. To improve the quality of the PECs, core-valence correlation and relativistic corrections are included. Core-valence correlation corrections are included with a cc-pCVTZ basis set. Relativistic correction calculations are carried out using the third-order Douglas-Kroll Hamiltonian approximation at the level of a cc-pV5Z basis set. The spectroscopic parameters of four Λ -S states and ten Ω states are calculated. Excellent agreement is found between the present results and the measurements. Using the PECs obtained by the MRCI + Q/AV5Z + CV + DK + SO calculations, the $G(v)$, B_v and D_v are calculated for each vibrational state of each Ω state, and those of the first 30 vibrational states are reported for the $X^2\Pi_{1/2}$, $X^2\Pi_{3/2}$, $B^2\Pi_{1/2}$ and $B^2\Pi_{3/2}$ states of the $^{14}\text{N}^{32}\text{S}$ radical. The spectroscopic parameters of four Ω states of the $a^4\Pi$ and the $G(v)$, B_v and D_v of the $X^2\Pi_{1/2}$, $X^2\Pi_{3/2}$, $B^2\Pi_{1/2}$ and $B^2\Pi_{3/2}$ states reported here are expected to be reliable predicted results.

1 Introduction

The NS radical is a molecule of interest to interstellar as well as laboratory spectroscopy. On the one hand, it is of fundamental importance in the interstellar fields of nitrogen chemistry [1] and sulfur chemistry [2]. For example, it was first identified in Sg2 B2 [3], then was detected in cold dark [4,5] and in warm [6] interstellar clouds, and recently was observed in Comet Hale-Bopp [7]; on the other hand, the NS is also important in combustion chemistry and in solid-state chemistry since the $(\text{NS})_x$ polymers have metallic conductivity properties [8]. The NS has a $^2\Pi_r$ ground state, and thus possesses fine structure and Λ -doubling. Because of the quadrupole moment of N nucleus, the Λ -doubling levels are further split by hyperfine structure [7]. Therefore, each rotational transition consists of two sets of hyperfine components. These hyperfine rotation transitions have important applications in interstellar fields. To clarify the hyperfine structure of rotation transitions, accurate knowledge of the spin-orbit (SO) coupling splitting of the radical must be understood in detail. For the reason, the effect on the spectroscopic and molecular

properties of the NS radical by the SO coupling splitting has been widely investigated, especially in experiment.

The NS radical has been the topic of wide experimental interest for a long time. In history, Fowler and Bakker [9] in 1932 made the first observation on its spectrum. Zeeman [10] in 1951 remeasured these bands and accurately determined the energy splitting of the $X^2\Pi_{3/2,1/2}$ components for the first time. Barrow et al. [11] in 1954 performed the rotational analysis of the β band system, and obtained the spectroscopic parameters of seven Ω states. Smith and Meyer [12] in 1964 observed the emission spectrum in active nitrogen-sulfur compound flames, and evaluated the spectroscopic parameters of eight Ω states. Narasimham and Srikameswaran [13] in 1964 performed the vibrational and rotational analysis of the Λ -S state of $B^2\Pi$, and obtained the T_e , R_e , ω_e , $\omega_e x_e$, B_e and α_e of the $B^2\Pi_{3/2}$ and $B^2\Pi_{1/2}$. Subsequently, Narasimham and Subramanian [14] in 1969 observed the emission spectra of the β , γ and two new band systems, and re-evaluated the spectroscopic parameters of $B^2\Pi_{3/2,1/2}$ components. Amano et al. [15] in 1969 also observed the microwave spectrum of the NS radical, and studied the SO coupling effect between the $X^2\Pi_{3/2}$ and $X^2\Pi_{1/2}$ states. Narasimham and Balasubramanian [16] in 1971 reported

^a e-mail: scattering@sina.com.cn

the vibrational and rotational analysis of four band systems, and obtained the energy separation between $H^2\Pi_{3/2}$ and $H^2\Pi_{1/2}$ states. In addition, they also fitted the vibrational and rotational constants of $X^2\Pi_{3/2}$ state. Jenouvrier and Pascat [17] in 1973 observed the transitions of several band systems of the $^{14}N^{32}S$ radical in the 225–380 nm, and evaluated the spectroscopic parameters of the components involved. Narasimham et al. [18] in 1975 observed two new bands with an open structure at 268.7 and 270.3 nm, and obtained the energy separation between the two Ω states, $X^2\Pi_{3/2}$ and $X^2\Pi_{1/2}$. Vervloet and Jenouvrier [19] in 1976 observed the $C^2\Sigma^+-X^2\Pi$, $I^2\Sigma^+-X^2\Pi$, $E^2\Pi-X^2\Pi$, $J^2\Sigma^+-X^2\Pi$ and $F^2\Delta-X^2\Pi$ transitions of the $^{14}N^{32}S$ radical in the 175–240 nm, and fitted the spectroscopic parameters of several Ω states. Some accurate results of several splitting Ω states prior to 1979 were summarized by Huber and Herzberg [20].

After 1979, some new transitions have also been observed, and the spectroscopic parameters and molecular properties of the Ω states involved here have still been extensively investigated [21–27]. For example, Jenouvrier and Pascat [21] in 1980 reanalyzed the emission band of the $B^2\Pi-X^2\Pi$ transitions in the 250–565 nm. Anaconda et al. [22] in 1986 measured the millimeter wave spectra of the $NS(X^2\Pi)$ for the vibrational levels lower than six. Jeffries et al. [23] in 1989 used laser-induced fluorescence to study the $B^2\Pi$, $A^2\Delta$ and $C^2\Sigma^+$ electronic states of the radical. Ongstad et al. [24] in 1991 observed the emission from several excited states of the NS and the fluorescence from the $NS(B^2\Pi_{3/2,1/2})$. Anaconda [25] in 1993 observed the far-infrared laser magnetic resonance spectra of the radical at 570.6 μm . Saleck et al. [26] in 1995 investigated the millimeter wave spectra of the NS isotopomers. And Wang et al. [27] in 2007 reported the resonance-enhanced multiphoton ionization spectroscopy on the $B^2\Sigma^+$ and $B^2\Pi$ states. Some spectroscopic parameters and molecular constants of several Ω states involved were fitted from these investigations [21–27].

In theory, the early ab initio work on the NS radical was performed by O'Hare [28] in 1970, who determined the ground-state dissociation energy by the Hartree-Fock-Roothaan ab initio calculations. Subsequently, Bialski and Grein [29] in 1976 made the first ab initio calculations on several low-lying excited states of the NS using the configuration interaction (CI) and minimal basis sets of Slater-type orbitals. From then on, a number of ab initio calculations [8,30–40] have been done, in which various spectroscopic parameters have been determined. Of these calculations [8,28–40], to our surprise, only two groups [36,40] investigated the SO coupling splitting, though a number of experiments [10–19,21,22,24–27] have been performed to study the energy splitting of several Λ -S states. In detail, one theoretical work is made by Kalcher [36] in 2002, who obtained the energy splitting of the $X^2\Pi$ state. The other is carried out by Ben Yaghlane et al. [40] in 2005, who determined the energy splitting of the two Λ -S states, $X^2\Pi$ and $a^4\Pi$.

The core-valence correlation and relativistic corrections have important effects on the accurate prediction

of the spectroscopic parameters and molecular constants even for small molecules such as NS. On the one hand, when we summarize the theoretical spectroscopic and molecular properties in the literature [8,28–40], we find that only three calculations [37–39] included the core-valence correlation or relativistic effect. And the available results are only for the ground state. Thus more theoretical work should be done so as to improve the quality of the spectroscopic parameters, in particular for the T_e ; on the other hand, if we exclude the energy splitting mentioned above, no theoretical spectroscopic and molecular properties of the Ω states involved here can be found in the literature.

In the present work, the effect on the potential energy curves (PECs) of the NS radical by the SO coupling will be introduced in the calculations. We are interested here in one lowest $^4\Pi$ and three lowest $^2\Pi$ states of the radical. The reasons are of two-folds. One is that the effects on the three lowest $^2\Pi$ electronic states by the SO coupling have been extensively investigated in experiment [10–19,21,22,24–27], but few results can be found in theory. Therefore, to be compared with the measurements, some theoretical work should be done. The other is that few theoretical results exist for the lowest $^4\Pi$ state, and no accurate experimental values can be found in the literature.

This paper is organized as follows. The PECs of four Λ -S ($X^2\Pi$, $a^4\Pi$, $B^2\Pi$ and $H^2\Pi$) and ten Ω states ($X^2\Pi_{1/2,3/2}$, $a^4\Pi_{1/2,1/2,3/2,5/2}$, $B^2\Pi_{1/2,3/2}$ and $H^2\Pi_{1/2,3/2}$) of the radical are calculated for internuclear separations from about 0.10 to 1.11 nm. The calculations are made using the complete active space self-consistent field (CASSCF) method, which is followed by the internally contracted multireference CI (MRCI) approach [41,42]. The effects on the PECs by the core-valence correlation and relativistic corrections are included. The effect on the energy splitting by the core-electron correlations is discussed. To obtain more reliable PECs, the Davidson modification [43,44] based on the internally contracted MRCI (MRCI+Q) calculations is taken into account. The spectroscopic parameters are calculated for the four Λ -S and ten Ω states. The spectroscopic parameters are compared with those reported in the literature. With the PECs obtained by the MRCI+Q/aug-cc-pV5Z+DK+CV+SO calculations, the $G(v)$, B_v and D_v are calculated for each vibrational state of each Ω state. And those of the first 30 vibrational states are reported for the four Ω states ($X^2\Pi_{1/2}$, $X^2\Pi_{3/2}$, $B^2\Pi_{1/2}$ and $B^2\Pi_{3/2}$) of the non-rotation radical.

2 Computational details

For a given molecular system, the whole Hamiltonian can be expressed as follows,

$$\hat{H} = \hat{H}^{el} + \hat{H}^{so}, \quad (1)$$

where \hat{H}^{el} is the spin-free Hamiltonian. \hat{H}^{so} is the SO part of Breit-Pauli Hamiltonian. The Breit-Pauli SO operator

\hat{H}^{so} can be expressed as [45],

$$\hat{H}^{so} = \frac{1}{2\mu^2 c^2} \left[\sum_i \sum_\alpha \frac{Z_\alpha e^2}{r_{i\alpha}^3} \hat{I}_{i\alpha} \cdot \hat{S}_i - \sum_i \sum_j \frac{e^2}{r_{ij}^3} \hat{I}_{ij} \cdot (\hat{S}_i + 2\hat{S}_j) \right]. \quad (2)$$

Equation (2) contains both one- and two-electron terms. In equation (2), \hat{I} and \hat{S} are space and spin angular momentum operators,

$$\hat{I}_{i\alpha} = (r_i - R_\alpha) \times P_i, \quad (3)$$

$$\hat{I}_{ij} = (r_i - r_j) \times P_i, \quad (4)$$

where roman and greek subscripts refer to electrons and nuclei, respectively. And the other symbols have their usual meanings. For example, Z_α and e are nuclear and electronic charges, respectively. P_i is the momentum operator. $r_{i\alpha}$ is the distance between the i th electron and the α th nuclei, and r_{ij} is the distance between the i th and j th electron.

In equation (2), the first double sum is known as the one-electron and the second as the two-electron operators [46], respectively. Instead of taking all the two-electron contributions of the wavefunction explicitly into account, the most important two-electron contributions of SO operator are incorporated by means of an effective one-electron Fock operator. According to these, Berning et al. [47] presented an efficient method for the calculations of Breit-Pauli SO matrix elements for internally contracted MRCI wavefunction, which has been implanted in MOLPRO 2008.1 program package [48].

The PEC calculations of four Λ -S and ten Ω states are made by the CASSCF approach, which is followed by the internally contracted MRCI calculations [41,42]. Therefore, the CASSCF is used as the reference wavefunction for the internally contracted MRCI calculations. The basis set used for the PEC calculations of four Λ -S states is the augmented correlation-consistent polarized aug-cc-pV5Z (AV5Z) set [49–51]. The PEC calculations of four Λ -S and ten Ω states are performed in the MOLPRO 2008.1 program package [48]. As we know, MOLPRO only uses Abelian point group symmetry, while the NS radical belongs to $C_{\infty v}$ symmetry. Therefore, to conveniently make the present calculations in MOLPRO 2008.1 program package, we substitute $C_{\infty v}$ symmetry with the C_{2v} subgroup by orienting the NS radical along the Z axis. In the calculations, eight molecular orbitals (MOs) are put into the active space, including four a_1 two b_1 and two b_2 symmetry MOs which correspond to the $3s3p$ shell of S and $2s2p$ shell of N atoms. The rest of the electrons in the NS radical are put into the closed-shell orbitals, including four a_1 , one b_1 and one b_2 symmetry MOs. The outmost $2p^3$ electrons of N and $3p^4$ electrons of S are in placed in the active space. Therefore, this active space is referred to as CAS (7, 8). When we use these MOs ($8a_1$ $3b_1$ and $3b_2$) to perform the PEC calculations, we find

that the PECs are smooth over the present internuclear separation range.

To accurately determine the PECs of four Λ -S and ten Ω states, the point spacing intervals used here is 0.02 nm for each state, except near the equilibrium internuclear separation where the spacing is 0.002 nm. Here, the smaller step is adopted around the equilibrium position of each electronic state so that the properties of each PEC can be displayed more clearly. For internuclear separations from 0.10 to 1.11 nm, the obtained PEC of each state is convergent. It means that the two atoms, S and N, are completely separated at 1.11 nm. The convergence of each PEC for internuclear separations from 0.10 to 1.11 nm, clarifies that the dissociation energy D_e can be determined by the difference between the total energy of the radical at the internuclear equilibrium separation (which is obtained by fitting) and the energy sum of the atomic fragments, N and S, at 1.11 nm.

In order to accurately determine the spectroscopic parameters, the PECs of four Λ -S and ten Ω states are first fitted to the analytical form by cubic splines so that the corresponding ro-vibrational Schrödinger equation can be conveniently solved. In this paper, we solve the ro-vibrational Schrödinger equation using Numerov's method [52]. That is, the ro-vibrational constants are first determined in a direct forward manner from the analytic potential by solving the ro-vibrational Schrödinger equation, and then the spectroscopic parameters are determined by fitting the vibrational levels obtained here.

3 Results and discussion

3.1 Effect on energy splitting by core-electron correlations

Using the theoretical method described in Section 2, we have studied the effect on the energy splitting and other spectroscopic parameters (T_e , R_e , ω_e and D_e) by the core-electron correlations. In this work, we use two all-electron basis sets, cc-pVTZ [49,50] and cc-pCVTZ [53,54], for the SO coupling calculations. The T_e , R_e , ω_e and D_e results determined by the MRCI + Q/AV5Z + SO calculations for the ten Ω states are collected in Table 1 together with the measurements [20,21] for comparison.

By comparison between the cc-pCVTZ and cc-pVTZ basis sets, we find that the addition of core-electron correlations does not yield any effect on the R_e of all the Ω states involved here. The effects on the ω_e by the addition of core-electron correlations are very small. For example, the ω_e difference between the cc-pCVTZ and cc-pVTZ basis sets is only 0.07 cm^{-1} for the $X^2\Pi_{3/2}$ and $X^2\Pi_{1/2}$ states. And the ω_e differences between the cc-pCVTZ and cc-pVTZ basis sets are also only 0.002 and 0.017 cm^{-1} for the $B^2\Pi_{3/2}$ and $B^2\Pi_{1/2}$ states, respectively. Such small differences of the R_e and ω_e can be ignored.

As illustrated in Table 1, the effects on the energy splitting of Ω states by including core-electron correlations are irregular. It obviously enlarges the splitting energies of $X^2\Pi_{3/2,1/2}$, $a^4\Pi_{5/2,3/2}$, $a^4\Pi_{3/2,1/2}$ and $a^4\Pi_{1/2,1/2}$ components, but produces very small change of splitting

Table 1. Spectroscopic parameters of the ten Ω states for the $^{14}\text{N}^{32}\text{S}$ radical obtained by the SO coupling at the MRCI+Q/AV5Z level.

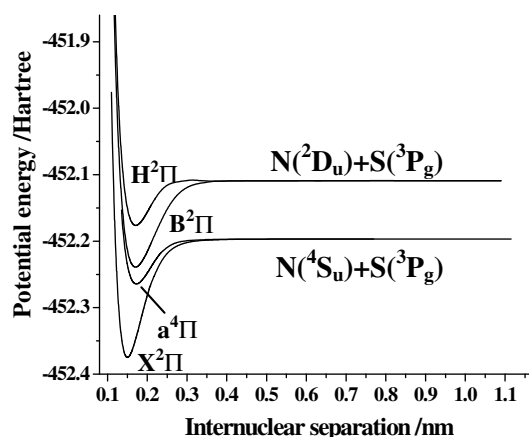
	cc-pCVTZ				cc-pVTZ			
	T_e/cm^{-1}	R_e/nm	w_e/cm^{-1}	D_e/eV	T_e/cm^{-1}	R_e/nm	w_e/cm^{-1}	D_e/eV
$X^2\Pi_{1/2}$	0.0	0.15002	1211.53	4.8510	0.0	0.15002	1211.46	4.8508
Exp. [20]	0.0	0.14940	1218.7	4.8753				
$X^2\Pi_{3/2}$	223.64	0.15002	1211.01	4.8394	221.79	0.15002	1211.08	4.8397
Exp. [20]	221.5	0.14940	1218.7	4.8478				
Exp. [21]	222.98	0.14901	1218.90					
$a^4\Pi_{1/2}$	24221.88	0.17263	736.248	1.8468	24227.80	0.17263	736.140	1.8460
$a^4\Pi_{1/2}$	24329.64	0.17260	736.554	1.8399	24327.67	0.17260	736.518	1.8396
$a^4\Pi_{3/2}$	24437.40	0.17258	736.910	1.8330	24427.53	0.17258	736.912	1.8333
$a^4\Pi_{5/2}$	24545.16	0.17255	737.216	1.8261	24527.61	0.17255	737.294	1.8270
$B^2\Pi_{1/2}$	29888.93	0.17036	794.887	3.5242	29882.57	0.17036	794.904	3.5234
Exp. [20]	30294.9	0.1697	797.31	3.5026				
$B^2\Pi_{3/2}$	29981.33	0.17025	797.104	3.5427	29975.63	0.17025	797.102	3.5419
Exp. [20]	30384.1	0.1697	798.78	3.4915				
$H^2\Pi_{1/2}$	43775.97	0.17083	770.336	1.8306	43769.83	0.17083	770.334	1.8307
Exp. [20]	44049	0.1702	767.6	1.7973				
$H^2\Pi_{3/2}$	43595.78	0.17088	769.487	1.8234	43590.08	0.17088	769.502	1.8234
Exp. [20]	43876	0.1702	767.6	1.8187				

energy of the $H^2\Pi_{3/2}$ and $H^2\Pi_{1/2}$ states. As to the splitting energy of the $B^2\Pi_{3/2}$ and $B^2\Pi_{1/2}$ states, core-electron correlations only make it slightly large. On the whole, core-electron correlations make the T_e closer to the experimental data. In conclusion, core-electron correlations only slightly improve the quality of spectroscopic parameters.

3.2 Results and analysis of the Λ -S states

The PECs are obtained by the MRCI+Q/AV5Z calculations for the $X^2\Pi$, $a^4\Pi$, $B^2\Pi$ and $H^2\Pi$ states of the radical. To clearly demonstrate the dissociation relationship of the four Λ -S states, we depict the PECs obtained by the MRCI+Q/AV5Z calculations in Figure 1. For the $X^2\Pi$ and $a^4\Pi$ states, the dissociation limit is $N(^4S_u) + S(^3P_g)$. For the $B^2\Pi$ and $H^2\Pi$ states, the dissociation limit is $N(^2D_u) + S(^3P_g)$. The present energy difference of 19229 cm^{-1} between the $N(^2D_u)$ and $N(^4S_u)$ atomic states is in excellent agreement with the experimental result of 19231 cm^{-1} .

Core-valence correlation and relativistic corrections have important effects on the PECs when we carry out the high-quality quantum chemistry calculations. To obtain more reliable PECs and then derive the accurate spectroscopic results, we must include the core-valence correlation and relativistic corrections into the PEC calculations. In this work, core-valence correlation corrections are included by using a cc-pCVTZ basis set [53,54]. Relativistic corrections are made using the third-order Douglas-Kroll Hamiltonian (DKH3) approximation [55–57] at the level of a cc-pV5Z basis set [58]. With the PECs determined by the

**Fig. 1.** PECs of four Λ -S states of NS radical by MRCI+Q/AV5Z calculations.

MRCI+Q/AV5Z+CV+DK calculations, the spectroscopic parameters of four Λ -S states are evaluated by the theoretical method described in Section 2. We collect the spectroscopic parameters in Table 2 together with some selected theoretical [31–33,35–40] and experimental [10,15,16,21,23] results for convenient comparison.

A number of calculations [8,28–40] have been performed to determine the spectroscopic results of these Λ -S states. As shown in Table 2, on the whole, the present spectroscopic parameters are in excellent agreement with the measurements [10,15,16,21,23] when compared with the theoretical ones [8,28–40]. For example, for the ground state, the D_e and ω_e deviate from the measurements only by 0.0249 eV [15] and 2.33 cm^{-1} [23]. No other theoretical D_e and ω_e values are closer to the experimental

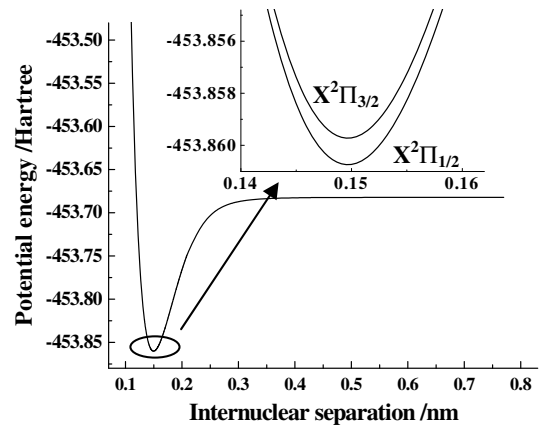
Table 2. Comparison of the spectroscopic parameters determined by MRCI + Q/AV5Z + CV + DK calculations with the experimental and other theoretical results.

	T_e/cm^{-1}	R_e/nm	ω_e/cm^{-1}	$\omega_e x_e/\text{cm}^{-1}$	$10^3 \omega_e y_e/\text{cm}^{-1}$	B_e/cm^{-1}	$10^3 \alpha_e/\text{cm}^{-1}$	D_e/eV
$X^2\Pi$	0.0	0.14962	1216.17	7.28259	15.9446	0.77323	6.25183	4.8504
Exp. [10]	0.0	0.14957	–	–	–	0.77364	6.12	
Exp. [15]	0.0	0.14938 ± 0.00002	–	–	–	–	4.8753	
Exp. [23]	0.0	–	1218.50 ± 2.5	7.24 ± 0.34	7 ± 11	(cubic fit)		
Cal. [33]	0.0	0.1495	1205					
Cal. [35]	0.0	0.14952	1279	7.69	–	–	6.42	6.301
Cal. [36]	0.0	0.15058	1202.4	7.24	–	0.742 (CAS-ACPF/cc-pVQZ)		
Cal. [37]	0.0	0.14938	1204	6.8				
Cal. [38]	0.0	0.15022	1229.36	8.230	–	–	5.36	4.9068
Cal. [39]	0.0	0.14940	1217.4					
Cal. [40]	0.0	0.1501	1203.4	6.24	63.8	0.767	5.6 (MRCI + Q/CC-pV5Z)	
$a^4\Pi$	24541.87	0.17227	735.972	5.74006	31.0541	0.58327	6.09261	1.8082
Exp. [21]	~ 27005	0.175	~ 760	~ 4	–	~ 0.56		
Cal. [31]	21369	0.1818	465					
Cal. [32]	22583.51	0.1734	782.1	–	–	0.5757		
Cal. [40]	$23809.48(T_0)$	0.1726	843.04	6.05	155.8	0.756	8.5	
$B^2\Pi$ ($2^2\Pi$)	30245.14	0.16995	797.649	3.71627	1.20163	0.59917	5.08302	3.5053
Exp. [16]	30328.5	0.1703	800	–	–	–	–	3.4984
Cal. [31]	31712	0.1753	428					
Cal. [32]	31374.95	0.1698	794.7	–	–	0.6002		
$H^2\Pi$ ($3^2\Pi$)	44022.88	0.17051	770.574	4.98055	35.3816	0.59513	5.67885	1.8046
Exp. [16]	43941 ± 5	$0.1705(r_0)$	813 ± 10	–	–	–	–	1.8107
Cal. [31]	48494	0.1838	728					
Cal. [32]	45650.96	0.1696	726.0	–	–	0.6018		

results [15,23] than the present ones. For the $B^2\Pi$ electronic state, the T_e , R_e , ω_e and D_e deviate from the experimental results [16] only by 83.36 cm^{-1} , 0.00035 nm, 2.351 cm^{-1} and 0.0069 eV. No other theoretical values are closer to the measurements [16] than the present ones. For the $H^2\Pi$ electronic state, the T_e , R_e , ω_e and D_e deviate from the experimental ones [16] only by 81.88 cm^{-1} , 0.00001 nm, 42.426 cm^{-1} and 0.0061 eV, respectively. No other theoretical values are closer to the measurements [16] than the present ones. Such comparison shows that the present spectroscopic results collected in Table 2 are of high quality. For the reason, the spectroscopic parameters of ten Ω states are calculated based on the PECs obtained by the MRCI + Q/AV5Z + CV + DK calculations.

3.3 Results and analysis of the Ω states

The SO coupling effect causes the present four Λ -S states split into ten Ω states. The spectroscopic results determined by the MRCI + Q/AV5Z + CV + DK + SO calculations are collected in Table 3 together with some measurements [11–14,17,20,21,27] for convenient comparison. The PECs of each Λ -S state obtained by the MRCI + Q/AV5Z + CV + DK calculations and its splitting Ω states obtained by the MRCI + Q/AV5Z + CV + DK + SO calculations are plotted in Figures 2–5, respectively. It should be noted that the SO coupling calculations collected in Table 3 and plotted in Figures 2–5 are performed by the all-electron

**Fig. 2.** PECs of the $X^2\Pi$ state and its two Ω states, $X^2\Pi_{3/2}$ and $X^2\Pi_{1/2}$.

cc-pCVTZ basis set. In addition, some splitting energies (not collected in Tab. 3) are gathered in Table 4 so that comparison can be roundly made between the available results and the present ones obtained by the all-electron basis sets, cc-pCVTZ and cc-pVTZ.

3.3.1 The $X^2\Pi$ electronic state

Our present internally contracted MRCI + Q calculations indicate that the Λ -S state of $X^2\Pi$ splits into two Ω states, $X^2\Pi_{3/2}$ and $X^2\Pi_{1/2}$, which can be clearly seen in Figure 2. The results of our calculations also indicate that

Table 3. Spectroscopic parameters of components of the X²Π, a⁴Π, B²Π and H²Π electronic states for the ¹⁴N³²S species determined by the MRCI + Q/AV5Z + CV + DK + SO calculations.

	T_e/cm^{-1}	R_e/nm	ω_e/cm^{-1}	$\omega_e x_e/\text{cm}^{-1}$	$10^3 \omega_e y_e/\text{cm}^{-1}$	B_e/cm^{-1}	$10^3 \alpha_e/\text{cm}^{-1}$	D_e/eV
X ² Π _{1/2}	0.0	0.14962	1216.43	7.27816	16.3692	0.77320	6.24794	4.8562
Exp. [11]	0.0	0.14957	1219.1	7.5	–	0.77364	6.12	
Exp. [12]	0.0	0.1496	1219	7.5	–	0.7736	6.1	
Exp. [17]	0.0	0.14955	1219.14	7.28	–	0.7730	6.3	
Exp. [20]	0.0	0.14940	1218.7	7.28	–	0.76960	6.35	4.8753
Exp. [21]	0.0	0.14955	1218.97	7.26	5.3	0.7730	6.3	
Exp. [27]	0.0	0.14931	1218.1	7.20	–	0.7758	6.5	
X ² Π _{3/2}	223.64	0.14962	1215.93	7.29887	15.6959	0.77326	6.26216	4.8446
Exp. [11]	223.03(T ₀)	0.14957	1219.1	7.5	–	0.77364	6.12	
Exp. [12]	223(T ₀)	0.1496	1219	7.5	–	0.7736	6.1	
Exp. [17]	223.15	0.14901	1218.90	7.34	–	0.7777	6.4	
Exp. [20]	221.5	0.14940	1218.7	7.28	–	0.77516	6.35	4.8478
Exp. [21]	222.98	0.14901	1218.90	7.30	5.3	0.7777	6.4	
Exp. [27]	220.4	0.14884	1218.0	7.05	–	0.7807	6.3	
a ⁴ Π _{1/2}	24492.05	0.17231	735.485	5.75913	37.2708	0.58300	6.08509	1.8185
a ⁴ Π _{1/2}	24599.59	0.17229	735.801	5.74007	31.8949	0.58318	6.08986	1.8116
a ⁴ Π _{3/2}	24707.36	0.17226	736.156	5.75422	34.0050	0.58336	6.09307	1.8047
a ⁴ Π _{5/2}	24814.90	0.17223	736.472	5.73886	30.0924	0.58354	6.09637	1.7978
B ² Π _{1/2}	30309.67	0.17000	796.329	3.73019	0.86655	0.59876	5.09337	3.4966
Exp. [12]	30105(T ₀)	0.168	800.4	–	0.612	–	–	–
Exp. [13]	30292.3	0.1713	797.00	3.63	–	0.5898	4.1	–
Exp. [14]	30297.9	0.17064	796.3	3.63	–	0.5962	4.8	–
Exp. [20]	30294.9	0.1697	797.31	3.72	–	0.5962	4.8	3.5026
Exp. [21]	29687.19	0.17064	797.35	3.72	–	0.5962	–	–
B ² Π _{3/2}	30401.19	0.16989	798.545	3.60091	6.90116	0.59942	4.99328	3.5152
Exp. [12]	30190(T ₀)	0.168	800	4	–	0.612	–	–
Exp. [13]	30364.8	0.1694	803.3	3.82	–	0.6030	4.8	–
Exp. [14]	30363.3	0.17068	803.3	3.82	–	0.5959	4.1	–
Exp. [20]	30384.1	0.1697	798.78	3.59	–	0.6013	4.6	3.4915
Exp. [21]	29778.29	0.16961	798.70	3.58	–	0.6013	–	–
H ² Π _{3/2}	44046.36	0.17053	770.194	5.01563	32.5060	0.59506	5.74226	1.8008
Exp. [20]	43876	0.1702	767.6	5.0	–	0.5915	5.9	1.8187
H ² Π _{1/2}	44226.11	0.17048	771.080	4.98728	35.5145	0.59531	5.67794	1.8080
Exp. [20]	44049	0.1702	767.6	5.0	–	0.5972	5.9	1.7973

Table 4. Comparison of the present SO coupling constants obtained by the MRCI + Q/AV5Z + CV + DK + SO calculations with the available measurements and other theoretical ones.

	This work ^a	This work ^b	Exp. [5]	Exp. [16]	Exp. [17]	Exp. [18]	Exp. [22]	Exp. [24]	Exp. [25]	Cal. [36]	Cal. [40]
X ² Π	223.64	211.79	223.15	223.03 ^[10]	223.15	221.4	223.37	223.37 ^[26]	223.0(A ₀)	215.0	204.6
a ⁴ Π	107.76	99.86	–	–	–	–	–	–	–	–	101.6
B ² Π	91.52	92.40	–	72.8	90.4	–	–	90(A ₀)	–	–	–
H ² Π	–179.75	–179.53	–	–172.4(A ₀)	–175.8(A ₀)	–	–175.69(A ₀) ^[19]	–	–	–	–

^aSO coupling correction is calculated by the (all-electron cc-pCVTZ) basis set.

^bSO coupling correction is calculated by the (all-electron cc-pVTZ) basis set.

the X²Π_{3/2} level lies above the X²Π_{1/2}, so that the X²Π_{1/2} is the ground state. As we know, the X²Π state of NS radical is characterized mainly by the open-shell electronic configuration 1σ²2σ²3σ²4σ²1π⁴5σ²6σ²7σ²2π⁴3π¹, where there is only one electron in the 3π shell. That is, it is a “less than half-filled” state. According to Hund’s second rule: when the highest energy shell is less than or equal to half-filled, the smaller J is the lower energy, and the result is opposite when the highest energy shell is more than half-filled. Obviously, our result is consistent with the rule.

For the X²Π state, the computed splitting energy by the all-electron cc-pCVTZ basis set is 223.64 cm^{−1}, which is larger than the recent measurements [26], 223.37 cm^{−1}, only by 0.27 cm^{−1}. In addition, the splitting energy calculated by the all-electron cc-pVTZ basis set is 211.79 cm^{−1}, which is also in excellent agreement with the measurements [26]. We notice that a number of experiments [10–12,16–22,24–27] have been done to determine the splitting energy of the X²Π_{3/2} and X²Π_{1/2} states. In these experiments, all the splitting energies are within 220.4–223.37 cm^{−1}. In theory, only two groups of splitting

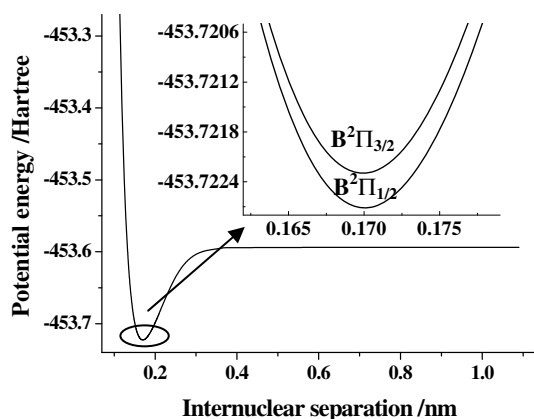


Fig. 3. PECs of the $B^2\Pi$ state and its two Ω states, $B^2\Pi_{3/2}$ and $B^2\Pi_{1/2}$.

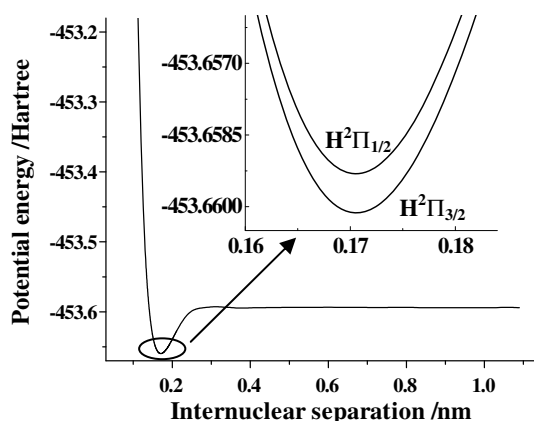


Fig. 4. PECs of the $H^2\Pi$ state and its two Ω states, $H^2\Pi_{3/2}$ and $H^2\Pi_{1/2}$.

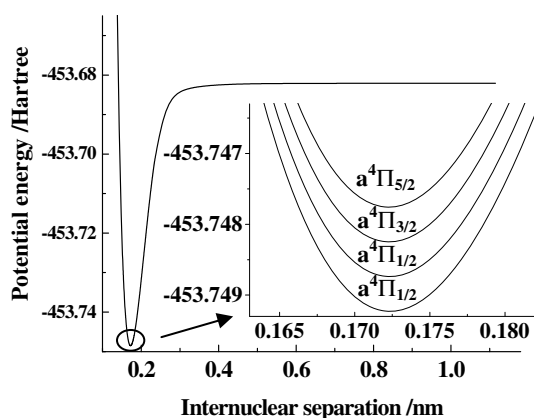


Fig. 5. PECs of the $a^4\Pi$ state and its four Ω states, $a^2\Pi_{5/2}$, $a^2\Pi_{3/2}$, $a^2\Pi_{1/2}$ and $a^2\Pi_{1/2}$.

energies can be found. One is 215.0 cm^{-1} , which was given by Kalcher [36] in 2002 at the CAS-ACPF level of theory. The other is 204.6 cm^{-1} , which was calculated by Ben Yaghlane et al. [40] in 2005 at the internally contracted MRCI + Q level of theory. Obviously, the two splitting energies [36,40] are slightly inferior to the present ones when compared with the available experimental data.

As seen in Table 3, the $X^2\Pi_{3/2}$ and $X^2\Pi_{1/2}$ states have the same equilibrium bond length, 0.14962 nm , which is exactly equal to that of the $X^2\Pi$ state. Therefore, the inclusion of SO coupling does not produce any effect on the R_e . As shown in Table 3, the recent R_e measurements [21] of $X^2\Pi_{3/2}$ and $X^2\Pi_{1/2}$ states are 0.14901 and 0.14955 nm . And the deviations of the present results from the measurements [21] are only 0.00061 nm (0.41%) and 0.00007 (0.05%), respectively. Our dissociation energies D_e are calculated to be 4.8446 and 4.8562 eV for the $X^2\Pi_{3/2}$ and $X^2\Pi_{1/2}$ states, which are still in good agreement with the those collected in reference [20], 4.8478 and 4.8753 eV , and the differences between the present results and the measurements [20] are only 0.0032 eV (0.07%) and 0.0191 (0.39%), respectively. To some extent, the inclusion of the SO coupling can improve the quality of the D_e . As to the ω_e , our computed values are 1215.93 and 1216.43 cm^{-1} for the $X^2\Pi_{3/2}$ and $X^2\Pi_{1/2}$, respectively, which are in reasonable agreement with all the measurements collected in Table 3. From the discussion made here, we can see that the SO coupling have little effects on the R_e and ω_e , but significantly make the D_e closer to the measurements [20]. In summary, for the $X^2\Pi_{3/2}$ and $X^2\Pi_{1/2}$ states, the present calculations can yield the encouraging spectroscopic results. Unfortunately, no other theoretical R_e , ω_e and D_e can be found for the splitting Ω states in the literature to the best our knowledge. Therefore, we can not compare the present results with other theoretical ones.

3.3.2 The $B^2\Pi$ electronic state

The PECs of A-S state of $B^2\Pi$ and its two splitting Ω states are depicted in Figure 3. The electronic configuration of $B^2\Pi$ state is $1\sigma^2 2\sigma^2 3\sigma^2 4\sigma^2 1\pi^4 5\sigma^2 6\sigma^2 7\sigma^2 2\pi^3 3\pi^2$. The electron transfer in this state is $2\pi^4 3\pi^1 \rightarrow 2\pi^3 3\pi^2$. As expected, the SO coupling splits the $B^2\Pi$ state into two components, $B^2\Pi_{3/2}$ and $B^2\Pi_{1/2}$. At the internuclear position, for the MRCI + Q/cc-pCVTZ calculations with the SO coupling excluded, the total energy of $B^2\Pi$ state is $-452.571471E_h$. For the MRCI + Q/cc-pCVTZ calculations with the SO coupling included, the total energies of the $B^2\Pi_{3/2}$ and $B^2\Pi_{1/2}$ states are -452.571263 and $-452.571692E_h$, respectively. Therefore, the $B^2\Pi_{1/2}$ state has a lower energy than the $B^2\Pi_{3/2}$. As shown in Table 3, the calculated splitting energy is 91.52 cm^{-1} by the cc-pCVTZ basis set, which is in excellent agreement with the recent experimental one [21] of 91.1 cm^{-1} . We notice that the early experimental splitting energy selected by Huber and Herzberg [20] is 89.2 cm^{-1} . The present result deviates from it [20] only by 1.9 cm^{-1} . In addition, when we use the cc-pVTZ basis set to calculate the splitting energy of the $B^2\Pi$ state, as shown in Table 4, the result of 92.40 cm^{-1} is obtained at the MRCI + Q/AV5Z + CV + DK level of theory. Such result is slightly inferior to the one calculated by the cc-pCVTZ basis set by comparison with the measurements [20,21].

As seen from Table 3, the excitation energy terms T_e of $B^2\Pi_{3/2}$ and $B^2\Pi_{1/2}$ states are 30401.19 and

30309.67 cm^{-1} , respectively, which agree favorably with the experimental findings [13,14,17,20]. The largest deviations from the measurements [13,14,17,20] are 37.89 cm^{-1} [14] for the $\text{B}^2\Pi_{3/2}$ state and 17.37 cm^{-1} [13] for the $\text{B}^2\Pi_{1/2}$ state. As shown in Table 2, the T_e of the $\text{B}^2\Pi$ state without the SO coupling is 30245.14 cm^{-1} , which deviates from the measurements [16] by 83.36 cm^{-1} . Therefore, the inclusion of the SO coupling correction can improve the quality of the T_e . The present dissociation energies D_e collected in Table 3 are 3.5152 eV for the $\text{B}^2\Pi_{3/2}$ and 3.4966 eV for the $\text{B}^2\Pi_{1/2}$ state, and the corresponding measurements [20] are 3.4915 and 3.5026 eV, respectively. The differences between them are 0.0237 (0.67%) for the $\text{B}^2\Pi_{3/2}$ and 0.006 eV (0.17%) for the $\text{B}^2\Pi_{1/2}$ state, respectively. On the whole, different from the ground state, the inclusion of the SO coupling correction has little effect on the D_e of the present Ω states. To our knowledge, no other theoretical results exist in the literature for the T_e and D_e of the two splitting Ω states, $\text{B}^2\Pi_{3/2}$ and $\text{B}^2\Pi_{1/2}$.

For the bond lengths of the $\text{B}^2\Pi_{3/2}$ and $\text{B}^2\Pi_{1/2}$ states, the present results are 0.16989 and 0.17000 nm, and the recent measurements [21] for the two states are 0.16961 and 0.17064 nm, respectively. The deviations of the present results from them [21] are only by 0.00028 (0.17%) for the $\text{B}^2\Pi_{3/2}$ and 0.00064 nm (0.38%) for the $\text{B}^2\Pi_{1/2}$ state. As to the ω_e , the present values are calculated to be 798.545 and 796.329 cm^{-1} for the $\text{B}^2\Pi_{3/2}$ and $\text{B}^2\Pi_{1/2}$ states, which deviates from the measurements [21] only by 0.155 (0.02%) and 1.021 (0.13%) cm^{-1} , respectively. In conclusion, the present spectroscopic results of the two splitting states agree well with the available experimental ones. In addition, different from the R_e , the inclusion of the SO coupling correction can make the ω_e of present splitting Ω states closer to the measurements [21].

3.3.3 The $\text{H}^2\Pi$ electronic state

The electronic configuration of $\text{H}^2\Pi$ state is $1\sigma^2 2\sigma^2 3\sigma^2 4\sigma^2 1\pi^4 5\sigma^2 6\sigma^2 7\sigma^2 2\pi^3 3\pi^2$. Similar to the $\text{B}^2\Pi$ electronic state, the electron transfer in the $\text{H}^2\Pi$ state is also $2\pi^4 3\pi^1 \rightarrow 2\pi^3 3\pi^2$. The SO coupling splits the $\text{H}^2\Pi$ state into two components, $\text{H}^2\Pi_{3/2}$ and $\text{H}^2\Pi_{1/2}$, and we depict the PECs of the $\text{H}^2\Pi$ and its two splitting Ω states in Figure 4. The results of our calculations indicate that the $\text{H}^2\Pi_{1/2}$ level lies above the $\text{H}^2\Pi_{3/2}$. For the energy separation between the $\text{H}^2\Pi_{3/2}$ and $\text{H}^2\Pi_{1/2}$ states, as tabulated in Table 4, the cc-pCVTZ basis set gives the result of -179.75 cm^{-1} , and the cc-pVTZ basis set gives the result of -179.53 cm^{-1} . The two results demonstrate that the core-electron correlations bring about little effect on the energy splitting. In addition, the two results agree well with the experimental ones of -175.69 [19] and -173 cm^{-1} [20].

As illustrated in Table 3, the bond lengths of $\text{H}^2\Pi_{3/2}$ and $\text{H}^2\Pi_{1/2}$ states are 0.17053 and 0.17048 nm, respectively, which are in excellent agreement with the experimental ones of 0.1702 nm selected by Huber and Herzberg [20]. The differences between them are only

0.00033 nm for the $\text{H}^2\Pi_{3/2}$ and 0.00028 nm for the $\text{H}^2\Pi_{1/2}$, respectively. By comparison with the R_e value without the SO coupling calculations, we find that the inclusion of SO coupling shortens the bond length of the $\text{H}^2\Pi_{1/2}$, whereas slightly lengthens the R_e of the $\text{H}^2\Pi_{3/2}$ state. As seen in Table 3, the present ω_e are calculated to be 770.194 and 771.080 cm^{-1} for the $\text{H}^2\Pi_{3/2}$ and $\text{H}^2\Pi_{1/2}$ states, respectively. The experimental result [20] without the SO coupling is 767.6 cm^{-1} , hence the deviations of our results from it are 2.594 (0.34%) and 3.48 cm^{-1} (0.45%), respectively. Similar to the bond lengths, the inclusion of the SO coupling slightly lowers the ω_e of the $\text{H}^2\Pi_{3/2}$, whereas slightly raise the ω_e of the $\text{H}^2\Pi_{1/2}$ state.

Although the splitting energy of Λ -S state of the $\text{H}^2\Pi$ agrees well with the experimental ones [19,20], the T_e of its two Ω states are only in general agreement with the measurements. In detail, the computed T_e of the $\text{H}^2\Pi_{3/2}$ and $\text{H}^2\Pi_{1/2}$ states are 44046.36 and 44226.11 cm^{-1} , respectively, while the corresponding measurements [20] are 43876 and 44049 cm^{-1} . And the differences between them are 170.36 (0.39%) and 177.11 cm^{-1} (0.40%), respectively. Different from the T_e , for the D_e of the $\text{H}^2\Pi_{3/2}$ and $\text{H}^2\Pi_{1/2}$ states, excellent agreement between the present results and the measurements [20] is found.

3.3.4 The $\text{a}^4\Pi$ electronic state

Except for the $\text{X}^2\Pi_{3/2}$, $\text{X}^2\Pi_{1/2}$, $\text{B}^2\Pi_{3/2}$, $\text{B}^2\Pi_{1/2}$, $\text{H}^2\Pi_{3/2}$ and $\text{H}^2\Pi_{1/2}$ states, we have also computed the splitting energies of the lowest $^4\Pi$ state of the NS radical, though no experimental results exist in the literature to this day. The electronic configuration of the $\text{a}^4\Pi$ state is $1\sigma^2 2\sigma^2 3\sigma^2 4\sigma^2 1\pi^4 5\sigma^2 6\sigma^2 7\sigma^2 2\pi^3 3\pi^2$. Similar to the Λ -S states of $\text{B}^2\Pi$ and $\text{H}^2\Pi$, the electron transfer in this state is still $2\pi^4 3\pi^1 \rightarrow 2\pi^3 3\pi^2$. The SO coupling effect splits the $\text{a}^4\Pi$ state into four components, $^4\Pi_{1/2}$, $^4\Pi_{1/2}$, $^4\Pi_{3/2}$ and $^4\Pi_{5/2}$. The results of our calculations indicate that the $\text{a}^4\Pi_{1/2}$ state has the lowest energy among the four components. For convenient comparison, we depict the PECs of the $\text{a}^4\Pi$ and its four splitting Ω states in Figure 5. We also collect the computed spectroscopic parameters in Tables 3 and 4, respectively.

Experimentally, the $\text{a}^4\Pi$ electronic state has been observed by Jenouvrier and Pascat [21], who reported its spectroscopic parameters (T_e , R_e , ω_e , $\omega_e x_e$ and B_e) in 1980. However, they [21] also stated that their spectroscopic parameters (T_e , ω_e , $\omega_e x_e$ and B_e) might be unreliable. Theoretically, at least four groups of spectroscopic results [29,31,32,40] have been published, but only one [40] is involved in the SO coupling splitting. As demonstrated in Tables 3 and 4, with the SO coupling included by the cc-pCVTZ basis set, the splitting energy of the two neighboring components is 107.76 cm^{-1} . And with the SO coupling included by the cc-pVTZ basis set, such result becomes about 99.86 cm^{-1} . Therefore, the inclusion of core-electron correlations into the SO coupling obviously enlarges the splitting energy of the $\text{a}^4\Pi$ state. In addition, Ben Yaghlane et al. [40] have calculated the SO coupling

constant of 101.6 cm^{-1} at the level of MRCI + Q/cc-pV5Z theory. As seen in Tables 2 and 3, the inclusion of the SO coupling makes the T_e of one Ω state ($a^4\Pi_{1/2}$) lower, while makes the T_e of three Ω states ($a^4\Pi_{1/2}$, $a^4\Pi_{3/2}$ and $a^4\Pi_{5/2}$) higher than that of the $a^4\Pi$ state.

As we know, on the one hand, the PECs of all the four Λ -S and ten Ω states are calculated by the same methods and the same basis sets, and the spectroscopic parameters of all the four Λ -S and ten Ω states are also evaluated by the same approach; on the other hand, the spectroscopic results of the four Λ -S states and the $X^2\Pi_{3/2,1/2}$, $B^2\Pi_{3/2,1/2}$ and $H^2\Pi_{3/2,1/2}$ components are in excellent agreement with the available measurements. According to these, we believe, with reason, that the spectroscopic parameters of the $a^4\Pi_{1/2}$, $a^4\Pi_{1/2}$, $a^4\Pi_{3/2}$ and $a^4\Pi_{5/2}$ states collected in Table 3 are reliable, though there are not any reliable measurements for comparison up to date. It is expected that the spectroscopic results tabulated in Table 3 can provide the useful guideline for future experimental or theoretical work.

3.4 Vibrational manifolds

By product, we have also calculated the vibrational manifolds using the PECs obtained here. To determine the vibrational manifolds, we must solve the radial Schrödinger equation of nuclear motion. In the adiabatic approximation, the radial Schrödinger equation of nuclear motion can be written as

$$\left[-\frac{\hbar^2}{2\mu} \frac{d^2}{dr^2} + \frac{\hbar^2}{2\mu r^2} J(J+1) + V(r) \right] \Psi_{v,J}(r) = E_{v,J} \Psi_{v,J}(r). \quad (5)$$

Here $V(r)$ is the PEC calculated here. r is the internuclear distance of the two atoms, N and S. μ is the reduced mass of the radical. v and J are the vibrational and rotational quantum numbers, respectively. $E_{v,J}$ and $\Psi_{v,J}(r)$ are the eigenvalues and eigenfunctions of the potential $J(J+1)\hbar/2\mu r + V(r)$, respectively. The rotational sublevel of a given vibrational level is represented by the following power series [59],

$$\begin{aligned} E_{v,J} = & G(v) + B_v[J(J+1)] - D_v[J(J+1)]^2 \\ & + H_v[J(J+1)]^3 + L_v[J(J+1)]^4 + M_v[J(J+1)]^5 \\ & + N_v[J(J+1)]^6 + O_v[J(J+1)]^7, \end{aligned} \quad (6)$$

where $G(v)$ is the vibrational level. B_v is the inertial rotation constant. And D_v , H_v , L_v , M_v , N_v and O_v are the centrifugal distortion constants. Using the PECs determined by the MRCI + Q/AV5Z + CV + DK + SO calculations, by solving equation (5) numerically, we have predicted the complete vibrational states for the ten Ω states. For each vibrational state of each Ω state, we have calculated its vibrational manifolds. Owing to the length limitation and avoiding congestion, here, we only tabulate the $G(v)$, B_v and D_v results of the first 30 vibrational states for the four Ω states ($X^2\Pi_{1/2}$, $X^2\Pi_{3/2}$, $B^2\Pi_{1/2}$ and $B^2\Pi_{3/2}$) of the non-rotation $^{14}\text{N}^{32}\text{S}$ radical and their

comparison with the available measurements [16,21] in Tables 5 and 6, respectively.

The $G(v)$, B_v and D_v results of the $X^2\Pi_{1/2}$ and $X^2\Pi_{3/2}$ states are very few in the literature. To the best of our knowledge, no theoretical results can be found in the literature, and only one group of experimental results was reported by Narasimham and Balasubramanian [16] in 1971. For convenient comparison, we collect the only experimental results [16] in Table 5. As shown in Table 5, the present rotational constants of the $X^2\Pi_{1/2}$ state are 0.744869 and 0.738522 cm^{-1} , whereas the corresponding experimental ones [16] are 0.74474 and 0.73836 cm^{-1} for $v = 4$ and 5 , respectively, hence the relative errors of our results are only 0.017% and 0.0022% .

Similar to those of the $X^2\Pi_{1/2}$ and $X^2\Pi_{3/2}$ states, the $G(v)$, B_v and D_v results of the $B^2\Pi_{1/2}$ and $B^2\Pi_{3/2}$ states are also few in the literature. In experiment, only one group of results [21] about the B_v can be found. And in theory, no results have been reported up to date. Here, we collect the present $G(v)$, B_v and D_v results together with the only experimental ones in Table 6 for convenient comparison. As seen in Table 6, the present results agree well with the only measurements. For example, for $v = 0$, 3 , 8 , 10 and 12 , the deviations of the present B_v from the measurements [21] are only by 0.41% , 0.29% , 0.26% , 0.16% and 0.93% for the $B^2\Pi_{1/2}$ state, and are also only by 0.97% , 0.85% , 0.45% , 0.78% and 0.49% for the $B^2\Pi_{3/2}$ state, respectively. These comparisons demonstrate that the present vibrational manifold calculations are of high quality.

As noted above, good agreement exists between the present spectroscopic results and experimental ones. And the rotational constants of the $X^2\Pi_{1/2}$, $B^2\Pi_{1/2}$ and $B^2\Pi_{3/2}$ states also agree favorably with the available experimental data. According to these, we believe that the $G(v)$, B_v and D_v collected in Tables 5 and 6 are reliable. They should be good predictions for future experimental or theoretical research.

4 Conclusions

The ten Ω states generated from the four Λ -S electronic states of NS radical are studied in detail for the first time. The internally contracted MRCI + Q method in combination with the AV5Z basis set is used to produce the PECs of four Λ -S states. To obtain more reliable PECs, core-valence correlation and relativistic corrections are considered in the present study. Core-valence correlation corrections are included using a cc-pCVTZ basis set. Relativistic correction calculations are performed using the third order Douglas-Kroll Hamiltonian approximation at the level of a cc-pV5Z basis set. The effects on the PECs by the SO coupling are treated by the Breit-Pauli Hamiltonian. With the PECs obtained by the MRCI + Q/AV5Z + CV + DK calculations, the spectroscopic parameters of the four Λ -S states are determined. With the PECs including all the corrections mentioned here, the spectroscopic parameters of ten Ω states

Table 5. Comparison of the present $G(v)$, B_v and D_v results obtained by MRCI + Q/AV5Z + DK + CV + SO calculations with the available measurements for the $X^2\Pi_{1/2}$ and $X^2\Pi_{3/2}$ states of the $^{14}\text{N}^{32}\text{S}$ radical.

v	$X^2\Pi_{1/2}$			$X^2\Pi_{3/2}$			
	$G(v)/\text{cm}^{-1}$	B_v/cm^{-1}	$10^6 D_v/\text{cm}^{-1}$	$G(v)/\text{cm}^{-1}$	B_v/cm^{-1}	$10^6 D_v/\text{cm}^{-1}$	
	This work	This work	Exp. [16]	This work	This work	This work	
0	606.44	0.770085	–	1.25195	606.17	0.770128	1.25325
1	1808.24	0.763800	–	1.25607	1807.43	0.763833	1.25742
2	2995.34	0.757508	–	1.26090	2993.97	0.757531	1.26233
3	4167.60	0.751201	–	1.26528	4165.65	0.751213	1.26675
4	5325.01	0.744869	0.74474	1.27028	5322.44	0.744870	1.27186
5	6467.47	0.738522	0.73836	1.27652	6464.24	0.738511	1.27822
6	7594.82	0.732152	–	1.28320	7590.90	0.732128	1.28494
7	8706.93	0.725749	–	1.28952	8702.28	0.725712	1.29147
8	9803.71	0.719319	–	1.29714	9798.30	0.719268	1.29912
9	10885.05	0.712859	–	1.30595	10878.83	0.712792	1.30816
10	11950.77	0.706358	–	1.31453	11943.70	0.706275	1.31682
11	13000.78	0.699820	–	1.32489	12992.81	0.699721	1.32740
12	14034.92	0.693233	–	1.33691	14025.99	0.693116	1.33965
13	15052.99	0.686600	–	1.34930	15043.06	0.686464	1.35217
14	16054.84	0.679908	–	1.36332	16043.85	0.679750	1.36649
15	17040.27	0.673150	–	1.37832	17028.18	0.672972	1.38166
16	18009.11	0.666323	–	1.39527	17995.84	0.666122	1.39898
17	18961.13	0.659417	–	1.41451	18946.63	0.659191	1.41840
18	19896.11	0.652423	–	1.43529	19880.31	0.652172	1.43933
19	20813.81	0.645335	–	1.45844	20796.65	0.645058	1.46305
20	21713.98	0.638142	–	1.48375	21695.39	0.637837	1.48850
21	22596.35	0.630837	–	1.51128	22576.27	0.630504	1.51633
22	23460.66	0.623410	–	1.54274	23439.02	0.623047	1.54819
23	24306.60	0.615833	–	1.57854	24283.34	0.615439	1.58431
24	25133.82	0.608100	–	1.61666	25108.87	0.607675	1.62284
25	25941.97	0.600197	–	1.66096	25915.26	0.599739	1.66734
26	26730.67	0.592098	–	1.70724	26702.14	0.591609	1.71367
27	27499.53	0.583824	–	1.75315	27469.13	0.583304	1.76008
28	28248.30	0.575371	–	1.80685	28215.99	0.574819	1.81419
29	28976.65	0.566700	–	1.86825	28942.37	0.566115	1.87603

involved here are calculated. The present spectroscopic parameters reproduce well the available experimental values. The effects on the energy splitting by the core-electron correlations are investigated using two all-electron basis sets, cc-pCVTZ and cc-pVTZ. The results illustrate that the core-electron correlations have small effect on the energy separations for the present states. Using the PECs determined by the MRCI + Q/AV5Z + CV + DK + SO calculations, the vibrational level inertial rotation and centrifugal distortion constants are calculated for each vibrational state of each Ω state, and those of the first 30 vibrational states are reported for the $X^2\Pi_{1/2}$, $X^2\Pi_{3/2}$, $B^2\Pi_{1/2}$ and

$B^2\Pi_{3/2}$ states of the $^{14}\text{N}^{32}\text{S}$ radical. The spectroscopic results of four Ω states of the $a^4\Pi$ and vibrational manifolds of the four Ω states reported here are expected to be reliable predicted results.

This work was sponsored by the National Natural Science Foundation of China under Grant Nos. 60777012, 61077073, 10874064, 61177092, 60977063 and 61127012 the Program for Science and Technology Innovation Talents in Universities of Henan Province in China under Grant No. 2008HA STIT008, the Innovation Scientists and Technicians Troop

Table 6. Comparison of the present $G(v)$, B_v and D_v results obtained by MRCI + Q/AV5Z + DK + CV + SO calculations with the available measurements for the $B^2\Pi_{1/2}$ and $B^2\Pi_{3/2}$ states of the $^{14}\text{N}^{32}\text{S}$ radical.

v	$B^2\Pi_{1/2}$			$B^2\Pi_{3/2}$				
	$G(v)/\text{cm}^{-1}$	B_v/cm^{-1}	$10^6 D_v/\text{cm}^{-1}$	$G(v)/\text{cm}^{-1}$	B_v/cm^{-1}	$10^6 D_v/\text{cm}^{-1}$		
	This work	This work	Exp. [21]	This work	This work	Exp. [21]	This work	
0	397.68	0.596326	0.5939	1.34815	399.02	0.597163	0.6030	1.34474
1	1186.52	0.591176	0.5895	1.33568	1190.54	0.592032	0.5978	1.33219
2	1967.83	0.586112	0.5905	1.32475	1974.57	0.586986	0.5938	1.32094
3	2741.55	0.581093	0.5794	1.31272	2751.08	0.582986	0.588	1.30902
4	3507.81	0.576156	–	1.30211	3520.15	0.577067	–	1.29807
5	4266.62	0.571255	–	1.29166	4281.84	0.572184	–	1.28776
6	5018.01	0.566415	–	1.28139	5036.13	0.567362	–	1.27756
7	5762.01	0.561625	–	1.27300	5783.06	0.562589	–	1.26891
8	6498.59	0.556871	0.5554	1.26527	6522.60	0.559851	0.5624	1.26138
9	7227.72	0.552151	0.5510	1.25800	7254.71	0.553145	0.5574	1.25408
10	7949.35	0.547457	0.5466	1.25141	7979.34	0.548466	0.5528	1.24770
11	8663.44	0.542786	0.542	1.24708	8696.44	0.543807	0.5485	1.24324
12	9369.90	0.538124	0.5432	1.24340	9405.93	0.541157	0.5438	1.23971
13	10068.64	0.533467		1.24388	10107.68	0.534513		1.23984
14	10759.46	0.528782		1.24466	10801.54	0.529841		1.24082
15	11442.18	0.524075		1.24798	11487.30	0.525146		1.24417
16	12116.60	0.519339		1.25115	12164.76	0.520420		1.24733
17	12782.54	0.514567		1.25740	12833.74	0.515659		1.25351
18	13439.78	0.509750		1.26440	13494.02	0.510852		1.26084
19	14088.13	0.504888		1.27329	14145.39	0.505999		1.26926
20	14727.37	0.499967		1.28397	14787.64	0.501087		1.28040
21	15357.28	0.494986		1.29678	15420.55	0.496114		1.29265
22	15977.62	0.489932		1.31165	16043.88	0.491068		1.30776
23	16588.16	0.484798		1.32924	16657.39	0.485944		1.32488
24	17188.62	0.479573		1.34961	17260.82	0.480729		1.34514
25	17778.74	0.474244		1.37281	17853.89	0.475412		1.36794
26	18358.21	0.468800		1.40052	18436.31	0.469980		1.39523
27	18926.72	0.463224		1.43158	19007.77	0.464419		1.42582
28	19483.92	0.457500		1.46746	19567.91	0.458711		1.46149
29	20029.45	0.451616		1.50726	20116.37	0.452843		1.50099

Construction Projects of Henan Province in China under Grant No. 08410050011, the Natural Science Foundation of Education Bureau of Henan Province in China under Grant No. 2010B140013 and Henan Innovation for University Prominent Research Talents in China under Grant No. 2006KYCX002.

References

1. E. Herbst, C.M. Leung, *Astrophys. J. Suppl. Ser.* **69**, 271 (1989)
2. E. Herbst, D.J. DeFrees, W. Koch, *Mon. Not. R. Astron. Soc.* **237**, 1057 (1989)
3. C.A. Gottlieb, J.A. Ball, E.W. Gottlieb, C.J. Lada, H. Penfield, *Astrophys. J.* **200**, L147 (1975)
4. D. McGonagle, W.M. Irvine, M. Ohishi, *Astrophys. J.* **422**, 621 (1994)
5. S.K. Lee, H. Ozeki, S. Saito, *Astrophys. J. Suppl. Ser.* **98**, 351 (1995) and references herein
6. D. McGonagle, W.M. Irvine, *Astrophys. J.* **477**, 711 (1997)
7. W.M. Irvine, M. Senay, A.J. Lovell, H.E. Matthews, D. McGonagle, R. Meier, *Icarus* **143**, 412 (2000)
8. R.C. Mawhinney, J.D. Goddard, *Inorg. Chem.* **42**, 6323 (2003)
9. A. Fowler, C.J. Bakker, *Proc. R. Soc. Lond. A* **136**, 28 (1932)
10. P.B. Zeeman, *Can. J. Phys.* **29**, 174 (1951)

11. R.F. Barrow, G. Drummond, P.B. Zeeman, Proc. Phys. Soc. A **67**, 365 (1954)
12. J.J. Smith, B. Meyer, J. Mol. Spectrosc. **14**, 160 (1964)
13. N.A. Narasimham, K. Srikameswaran, Proc. Ind. Acad. Sci. A **59**, 227 (1964)
14. N.A. Narasimham, T.K.B. Subramanian, J. Mol. Spectrosc. **29**, 294 (1969)
15. T. Amano, S. Saito, E. Hirota, Y. Morino, J. Mol. Spectrosc. **32**, 97 (1969)
16. N.A. Narasimham, T.K. Balasubramanian, J. Mol. Spectrosc. **40**, 511 (1971)
17. A. Jenouvrier, B. Pascat, Can. J. Phys. **51**, 2143 (1973)
18. N.A. Narasimham, K. Raghuvveer, T.K. Balasubramanian, J. Mol. Spectrosc. **54**, 160 (1975)
19. M. Vervloet, A. Jenouvrier, Can. J. Phys. **54**, 1909 (1976)
20. K.P. Huber, G. Herzberg, Molecular Spectra and Molecular Structure, in *Constants of Diatomic Molecules* (Van Nostrand Reinhold, New York, 1979), Vol. 4, and references herein
21. A. Jenouvrier, B. Pascat, Can. J. Phys. **58**, 1275 (1980)
22. J.R. Anaconda, M. Bogey, P.B. Davies, C. Demuynck, J.L. Destombes, Mol. Phys. **59**, 81 (1986)
23. J.B. Jeffries, D.R. Crosley, G.P. Smith, J. Phys. Chem. **93**, 1082 (1989)
24. A.P. Ongstad, R.I. Lawconnell, T.L. Henshaw, J. Chem. Phys. **97**, 1053 (1992)
25. J.R. Anaconda, Spectrochim. Acta A **50**, 909 (1994)
26. A.H. Saleck, H. Ozeki, S. Saito, Chem. Phys. Lett. **244**, 199 (1995)
27. T.T. Wang, C.Y. Li, X.F. Zheng, Y. Chen, Chin. Sci. Bull. **52**, 596 (2007)
28. P.A.G. O'Hare, J. Chem. Phys. **52**, 2992 (1970)
29. M. Bialski, F. Grein, J. Mol. Spectrosc. **61**, 321 (1976)
30. A. Karpfen, P. Schuster, J. Petkov, H. Lischka, J. Chem. Phys. **68**, 3884 (1978)
31. G.C. Lie, S.D. Peyerimhoff, R.J. Buenker, J. Chem. Phys. **82**, 2672 (1985)
32. S.P. Karna, F. Grein, J. Mol. Spectrosc. **120**, 284 (1986)
33. M. Herberhold, Comments Inorg. Chem. **7**, 53 (1988)
34. A.I. Boldyrev, N. Gonzales, J. Simons, J. Phys. Chem. **98**, 9931 (1994)
35. D.P. Chong, Chem. Phys. Lett. **220**, 102 (1994)
36. J. Kalcher, Phys. Chem. Chem. Phys. **4**, 3311 (2002)
37. L.R. Peebles, P. Marshall, Chem. Phys. Lett. **366**, 520 (2002)
38. J. Czernek, O. Živný, Chem. Phys. **303**, 137 (2004)
39. P.A. Denis, J. Phys. Chem. A **108**, 11092 (2004)
40. S. Ben Yaghlane, S. Lahmar, Z. Ben Lakhdar, M. Hochlaf, J. Phys. B: At. Mol. Opt. Phys. **38**, 3395 (2005)
41. H.-J. Werner, P.J. Knowles, J. Chem. Phys. **89**, 5803 (1988)
42. P.J. Knowles, H.-J. Werner, Chem. Phys. Lett. **145**, 514 (1988)
43. S.R. Langhoff, E.R. Davidson, Int. J. Quantum Chem. **8**, 61 (1974)
44. A. Richartz, R.J. Buenker, S.D. Peyerimhoff, Chem. Phys. **28**, 305 (1978)
45. H.A. Bethe, E. Salpeter, *Quantum Mechanics of One- and Two-Electron Atoms* (Plenum, New York, 1977)
46. D.G. Fedorov, M.S. Gordon, J. Chem. Phys. **112**, 5611 (2000)
47. A. Berning, M. Schweizer, H.-J. Werner, P.J. Knowles, P. Palmieri, Mol. Phys. **98**, 1823 (2000)
48. MOLPRO 2008.1 is a package of ab initio programs written by H.-J. Werner, P.J. Knowles, R. Lindh, F.R. Manby, M. Schütz, P. Celani, T. Korona, A. Mitrushenkov, G. Rauhut, T.B. Adler, R.D. Amos, A. Bernhardsson, A. Berning, D.L. Cooper, M.J.O. Deegan, A.J. Dobbyn, F. Eckert, E. Goll, C. Hampel, G. Hetzer, T. Hrenar, G. Knizia, C. Köppl, Y. Liu, A.W. Lloyd, R.A. Mata, A.J. May, S.J. McNicholas, W. Meyer, M.E. Mura, A. Nicklass, P. Palmieri, K. Pflüger, R. Pitzer, M. Reiher, U. Schumann, H. Stoll, A.J. Stone, R. Tarroni, T. Thorsteinsson, M. Wang, A. Wolf
49. D.E. Woon, T.H. Dunning, J. Chem. Phys. **98**, 1358 (1993)
50. T.H. Dunning, J. Chem. Phys. **90**, 1007 (1989)
51. T.V. Mourik, A.K. Wilson, T.H. Dunning, Mol. Phys. **96**, 529 (1999)
52. J.L.M.Q. González, D. Thompson, Comput. Phys. **11**, 514 (1997)
53. D.E. Woon, T.H. Dunning, J. Chem. Phys. **103**, 4572 (1995)
54. K.A. Peterson, T.H. Dunning, J. Chem. Phys. **117**, 10548 (2002)
55. M. Reiher, A. Wolf, J. Chem. Phys. **121**, 2037 (2004)
56. A. Wolf, M. Reiher, B.A. Hess, J. Chem. Phys. **117**, 9215 (2002)
57. M. Reiher, A. Wolf, J. Chem. Phys. **121**, 10945 (2004)
58. W.A. de Jong, R.J. Harrison, D.A. Dixon, J. Chem. Phys. **114**, 48 (2001)
59. G. Herzberg, *Molecular Spectra and Molecular Structure* (Van Nostrand Reinhold, New York, 1951), Vol. 1